For the above two cases, the frequency response (1) can be simplified by using $h(L+k) = h(L-k)$, i.e.,

$$\begin{aligned} H(\omega) &= \sum_{k=0}^{N-1} h(k)e^{-jk\omega} \\ &= e^{-jL\omega}\{h(L) + 2h(L-1)\cos(\omega) + \cdots + 2h(0)\cos(L\omega)\} \\ &= e^{-jL\omega}\sum_{k=0}^{L} \hat{h}(k)\cos(k\omega) \end{aligned} \tag{30}$$

where

$$\hat{h}(k) = \hat{h}_R(k) + j\hat{h}_I(k) = \begin{cases} h(L), & k = 0, \\ 2h(L-k), & k = 1, 2, \cdots, L. \end{cases} \tag{31}$$

Then the design problem becomes two real Chebyshev approximations, i.e., $\sum_{k=0}^{L} \hat{h}_R(k)\cos(k\omega)$ is used to approximate $\cos[L\omega + P(\omega)]$ and $\sum_{k=0}^{L} \hat{h}_I(k)\cos(k\omega)$ is used to approximate $\sin[L\omega + P(\omega)]$. Notice that these approximations are typical real FIR filter approximations, which can be achieved simply by the original Parks-McClellan program after slight modification even without using McCalling's algorithm.

Example 2 Design of Slant-Delay All-Pass Filter*:* In this example, an all-pass filter is designed with length 31 and the desired phase response as

$$P(\omega) = \begin{cases} -7\omega + \frac{4\omega^2}{\pi} - 11\pi, & -\pi \le \omega \le -0.5\pi \\ -15\omega - \frac{4\omega^2}{\pi} - 13\pi, & -0.5\pi \le \omega \le 0.5\pi \\ -23\omega - \frac{4\omega^2}{\pi} - 9\pi, & 0.5\pi \le \omega \le \pi. \end{cases} \tag{32}$$

Its desired group delay is

$$\tau(\omega) = -\frac{dP(\omega)}{d\omega} = \begin{cases} 7\omega - \frac{8\omega}{\pi}, & -\pi \le \omega \le -0.5\pi \\ 15\omega + \frac{8\omega}{\pi}, & -0.5\pi \le \omega \le 0.5\pi \\ 23\omega + \frac{8\omega}{\pi}, & 0.5\pi \le \omega \le \pi. \end{cases} \tag{33}$$

Fig. 2(a)–(c) shows the resultant magnitude response, group delay response and the trace of complex error, respectively. The related results are tabulated in Table I.

IV. Conclusion

By separately approximating the real and imaginary parts of an FIR filter with complex-valued frequency response, the Parks-McClellan-McCalling program can be slightly modified to design general complex FIR filters very effectively. Although the approach does not minimize the complex Chebyshev error, this approach has several practical advantages such as simplicity, fast design time and easy implementation with satisfactory performance. Design examples including single-passband filters and complex all-pass filters are presented to show the effectiveness of this approach.

References

[1] J. H. McClellan, T. W. Parks, and L. R. Rabiner, "A computer program for designing optimum FIR linear phase digital filters," *IEEE Trans. Audio Electroacoust*, vol. AU-21, pp. 506–526, Dec. 1973.

[2] M. T. McCalling, "Design of digital FIR filters with complex conjugate pulse responses," *IEEE Trans. Circuits Syst.*, vol. CAS-25, pp. 1103–1105, Dec. 1978.

[3] L. J. Karam and J. H. McClellan, "Complex Chebyshev approximation for FIR filter design," *IEEE Trans. Circuits Syst.*, pp. 207–216, Mar. 1995.

[4] X. Chen and T. W. Parks, "Design of FIR filters in the complex domain," *IEEE Trans. Acoust., Speech, Signal Processing*, vol. ASSP-35, pp. 144–153, Feb. 1987.

[5] K. Preuss, "On the design of FIR filters by complex Chebyshev approximation," *IEEE Trans. Acoust., Speech, Signal Processing*, vol. 37, pp. 702–712, May 1989.

[6] C.-Y. Tseng, "A numerical algorithm for complex Chebyshev FIR filter design," in *Proc. ISCAS-92*, 1992, pp. 549–552.

[7] D. Burnside and T. W. Parks, "Accelerated design of FIR filters in the complex domain," in *Proc. ICASSP-93*, May 1993, pp. 81–84.

[8] C.-Y. Tseng, "Further results on complex Chebyshev FIR filter design using a multiple exchange algorithm," in *Proc. ISCAS-93*, May 1993, pp. 343–346.

[9] ——, "An efficient implementation of Lawson's algorithm with application to complex Chebyshev FIR filter design," *IEEE Trans. Circuits Syst. II*, vol. 42, pp. 245–260, Apr. 1995.

[10] S. C. Pei and J. J. Shyu, "Design of real FIR filters with arbitrary complex frequency responses by two real Chebyshev approximations," *Signal Processing*, pp. 119–129, Jan. 1992.

[11] K. Steiglitz, "Design of FIR digital phase networks," *IEEE Trans. Acoust., Speech Signal Processing*, vol. ASSP-29, pp. 171–176, Apr. 1981.

A Digital Scattering Model of the Cochlea

Louiza Sellami and Robert W. Newcomb

***Abstract*— A cascade digital scattering linear model of the cochlea, suitable for Kemp echo cochlea characterization, is developed. This model stems from a unidimensional transmission line model in which nonuniform and loss properties are included. Its lattice structure is obtained by rephrasing the model equations in terms of incident and reflected scattering waves. A characterization of the cochlea, through the estimation of the width, the stiffness, and the damping of the basilar membrane, is made with the model and the results compared to data available in the literature.**

I. Introduction

Cochlea modeling, primarily in the frequency domain, has been the subject of many studies for decades and several models exist in the literature, each one describing one or more particular functional aspects of the cochlea. Most of these studies were focused on the filter-like frequency response of the basilar membrane (BM) to an acoustical sinusoidal stimulation. All of these primarily linear models are not directly appropriate for Kemp echo phenomenon, since the latter is based on the scattering behavior of incident and reflected pressure waves in the cochlea [1], [2]. Hence, a treatment in terms of scattering variables is the most relevant.

Kemp echoes are acoustical signals emitted by the ear as a result of acoustic stimulation. These emissions have been shown to possess characteristics which are modified by damage to the auditory system. Although of small magnitude, Kemp echoes can be isolated with proper filtering techniques. Because there are significant differences in the Kemp echoes for normal versus certain types of damaged ears, it is felt that the Kemp echoes could be a reliable noninvasive technique for demonstrating objectively the presence of normal activity in the cochlea, detecting changes in its functioning, as well as detecting hearing loss and other noncochlear damages. Since

Manuscript received July 27, 1995; revised February 19, 1996 and July 16, 1996. This paper was recommended by Associate Editor P. P. Civalleri.

The authors are with the Microsystems Laboratory, Electrical Engineering Department, University of Maryland, College Park, MD 20742 USA.

Publisher Item Identifier S 1057-7122(97)01497-9.

all humans lose some hearing due to aging, illness, or accidents, noninvasive screening of hearing and the diagnosis and treatment of hearing impairment should be very important to most of us. Kemp echoes appear to be a potential clinical tool for this purpose. Consequently, it is important to develop theoretical models of the ear that can simulate Kemp echoes in their impulse response and from which a characterization of the cochlea can be made.

This brief continues studies initiated by and with Gomez and Rodellar [3], [5], [6] but differs in two essential ways from past research. First, the model itself is different, in that it is of a scattering nature, i.e., based on incident and reflected pressure waves. Second, it extends the model of [3], [5]–[7] which converts to a cascade of digital scattering lattice sections with each lattice now described by a transfer scattering matrix containing the characteristic parameters of that section of the cochlea. The advantage of the proposed model structure is that it simulates Kemp echoes in their impulse response and leads to a systematic cochlea characterization directly from Kemp echoes, as is shown in Section IV.

The model is based on the unidimensional transmission line structure into which nonuniform and loss properties are incorporated. The model is first set up in the time-domain to include nonlinearities in the gradients of the pressure difference and the fluid velocity which are both dependent on the transversal displacement of the BM. Since for normal sound amplitude the maximum BM displacement is much smaller than its width, reasonable approximations can be made which lead to a linearized model. The lattice structure of the linearized model is obtained by rephrasing the model equations in terms of incident and reflected scattering waves and digitizing the resulting equations in both space and time. The generated structure is a cascade of digital lattice sections where each lattice corresponds to one section of the cochlea. The lattice sections are described in the z-domain by their transfer scattering matrices whose entries are functions of the geometrical and mechanical parameters of the cochlea, thus allowing a systematic extraction of these parameters.

II. Equations of the Model

For the purpose of describing Kemp echoes, the following simplifications are introduced into the model:

1) The cochlea is an isolated cavity, communicating with its surroundings through the windows only.
2) The fluid in the cochlea is incompressible and one-dimensional which implies that all the relevant quantities are functions of the longitudinal coordinate only.
3) The spiral coiling is ignored.
4) The cochlea is composed of two channels only, since the cochlea duct and Reissner's membrane can be considered geometrically and dynamically part of the BM. This assumption is based on the fact that the cochlea duct is much smaller than the other two scalae, and that Reissner's membrane vibrates in phase with the BM.
5) The cross-sectional areas of the two channels are equal and independent of time.
6) The BM is modeled mechanically as a cascade of second order linear systems, characterized by a mass assumed constant, stiffness, and damping. The BM vibrates transversally only.

The geometrical model, as indicated schematically in Fig. 1, represents an uncoiled one-dimensional cochlea with two chambers (vestibuli and tympani) filled with fluid (perilymph) and separated by the BM. The two chambers communicate with each other at the apex through the Helicotrema. The geometrical parameters are the average length L of the cochlea, the cross-sectional areas $S_V(x)$ and $S_T(x)$ of scala vestibuli and scala tympani, respectively, and the

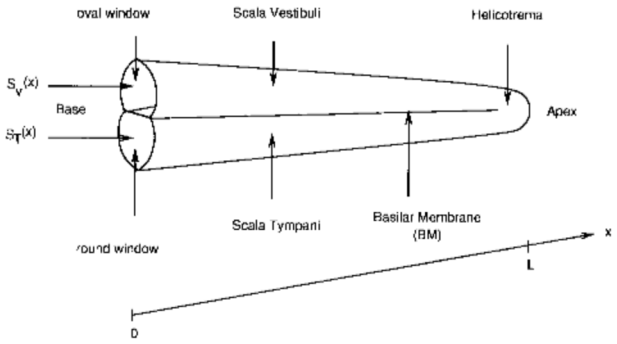

Fig. 1. Schematic drawing of an ideal unfolded cochlea.

TABLE I
The Geometrical and Mechanical Parameters of the Cochlea Measured by Various Authors. Here x is Measured in Centimeters. The Average Values Used for ρ_F, μ, and L are 1 $\mathrm{g/cm^3}$, 0.143 $\mathrm{g/cm^2}$, and 35 mm, Respectively

Author	Width $D(x)$ cm	Cross-sectional area $S_V(x)$ $\mathrm{cm^2}$	Damping $\sigma(x)$ $\mathrm{dyne.s.cm^{-3}}$	Stiffness $\phi(x)$ $\mathrm{dyne.cm^{-3}}$
Peterson	$0.019 + 0.0093x$	$0.029 - 0.005x$	–	$1.7210^8 e^{-2x}$
Zwislocki	–	$1.2510^{-2} e^{-.5x}$	$124e^{.25x}$	$2.510^8 e^{-1.5x}$
Lien	–	–	$94(x + .8)$	$4.7610^8 e^{-1.61x}$
Siebert	–	–	$5e^{2.25x}$	$210^8 e^{-1.5x}$
Allen	$0.017e^{.85x}$	–	$300e^{1.7x}$	$10^9 e^{-3.4x}$
Neely		–	200	$10^8 e^{-2x}$

width $D(x)$ of the BM. The mechanical parameters are the mass μ of the fluid, stiffness $\phi(x)$, and frictional resistance $\sigma(x)$ of the BM, all per unit area, and the fluid density ρ_F. The mass is mainly due to the fluid. The stiffness is almost completely determined by the transverse bending of the BM, as Reissner's membrane is one tenth as thick and is under no pressure. The resistance is due to the internal friction within the BM. The width, cross-sectional area, stiffness, and resistance of the human cochlea partition have been estimated in the literature and the results summarized in Table I [3], [4].

The equations of the pressure and fluid velocity describing the motion of the fluid and the BM, derived in this section and following a development in [3] and [7], are based on Newton's law for force on a fluid, conservation of mass, and the BM motion equation. We use $p_V(t,x)$ and $p_T(t,x)$ to designate the pressure waves in the fluid at time t and position x and $\vec{v}(t,x)$ the velocity of the fluid. By virtue of the taper and the closed nature of the cochlea, a velocity $\vec{v}_V$ in the scala vestibuli induces a velocity $\vec{v}_T$ in the scala tympani such that

$$\vec{v}_T(t,x) = -\vec{v}_V(t,x). \tag{1}$$

We take (1) as a basic assumption of the theory which allows us to primarily work with $\vec{v}_V$. Also, it is the pressure difference

$$p(t,x) = p_V(t,x) - p_T(t,x) \tag{2}$$

which causes the BM to vibrate transversally; thus, we will express our equations in terms of $p(t,x)$.

Newton's Law for Force on Cochlear Fluid

There are three forces (neglecting the gravitational force) acting on the fluid in the cochlea: the inertial force, due to the mass of the fluid, the frictional force, due to frictions in the fluid, and the restoring force, due to the pressure difference in the scalae. These forces are taken per unit length. Using Newton's law and the equality $d[\cdot]/dt = \partial[\cdot]/\partial t + [\cdot]\nabla[\cdot]$ [8, p. 240] for the fluids in the scalae

vestibuli and tympani, we have

$$\frac{\partial v_V(t,x)}{\partial t} + v_V(t,x)\nabla v_V(t,x) = \frac{-1}{\rho_F}[\nabla p_V(t,x) + R_V v_V(t,x)] \quad (3)$$

$$\frac{\partial v_T(t,x)}{\partial t} + v_T(t,x)\nabla v_T(t,x) = \frac{-1}{\rho_F}[\nabla p_T(t,x) - R_V v_V(t,x)] \quad (4)$$

where ∇ is the gradient operator with respect to x and R_V the frictional coefficient. Subtracting (4) from (3), using (2), and multiplying and dividing by $S_V(x)$ results in

$$\nabla p(t,x) = -\frac{2}{S_V(x)}\left[R_V[S_V(x)v_V(t,x)] + \rho_F \frac{\partial[S_V(x)v_V(t,x)]}{\partial t}\right]. \quad (5)$$

In (5) we have the gradient of the pressure difference as a function of time and displacement along the cochlea.

Conservation of Cochlear Fluid Mass

In this section we derive a similar equation for the fluid velocity, the end result being given by (15). We start with the well known mass conservation equation [8, p. 326]

$$\frac{d\rho_F(t,x)}{dt} = -\rho_F(t,x)\nabla\cdot\vec{v}(t,x) \quad \text{with} \quad \frac{d}{dt} = \frac{\partial}{\partial t} + \vec{v}\cdot\nabla \quad (6)$$

From the fluid incompressibility assumption, i.e., $d\rho_F/dt = 0$, it follows that

$$\nabla\cdot\vec{v}(t,x) = \lim_{\Delta V\to 0}\left\{\frac{\oint\!\!\oint_S \vec{v}(t,x)\cdot d\vec{S}}{\Delta V}\right\} = 0. \quad (7)$$

To evaluate the integral term in (7), we consider a section of length Δx of the scala vestibuli with a stiff outer wall. As a result, the velocity perpendicular to the upper external surface is zero. For this section, the integral of (7) is expanded as

$$\oint\!\!\oint_S \vec{v}(t,x)\cdot d\vec{S} = \iint_{S(x)} \vec{v}(t,x)\cdot d\vec{S} + \iint_{S(x+\Delta x)} \vec{v}(t,x)\cdot d\vec{S} + \iint_{S(BM)} \vec{v}(t,x)\cdot d\vec{S} \quad (8)$$

for which

$$\iint_{S(x)} \vec{v}(t,x)\cdot d\vec{S} = -S_V(x)v_V(t,x) \quad (9)$$

$$\iint_{S(x+\Delta x)} \vec{v}(t,x)\cdot d\vec{S} = S_V(x+\Delta x)v_V(t,x+\Delta x) \quad (10)$$

$$\iint_{S(BM)} \vec{v}(t,x)\cdot d\vec{S} = -2\Delta x\int_0^{D(x)/2}\dot{\xi}(t,x,y)\,ds \quad (11)$$

where (9) and (10) are obtained by using the fact that the velocity $\vec{v}_V$ is constant over the surface at x and similarly at $x+\Delta x$, and points in the opposite direction of $\vec{S}_V$ at x and in the same direction at $x+\Delta x$. In (11), $\dot{\xi}(t,x,y) = \partial\xi(t,x,y)/\partial t$ is the velocity of the BM and ds the differential arc length along the displaced BM approximated by

$$ds \approx \sqrt{(dy)^2 + (d\xi(t,x,y))^2} \quad (12)$$

where the "transverse" variable y is introduced solely for the purpose of approximating $\xi(t,x,y)$. To evaluate (11), we follow [3] and [7] and approximate $\xi(t,x,y)$ by the triangle of (13) since from physiological observations for normal sound amplitude, the maximum BM displacement $\xi_m(t,x)$, which is of the order of 10^{-6} cm, is much smaller than $D(x)/2$, of order 10^{-2} cm.

$$\xi(t,x,y) = \begin{cases} \dfrac{2\xi_m(t,x)}{D(x)}y & 0 \le y \le \dfrac{D(x)}{2} \\ \dfrac{-2\xi_m(t,x)}{D(x)}y + 2\xi_m(t,x) & \dfrac{D(x)}{2} \le y \le D(x). \end{cases} \quad (13)$$

Substituting (12) in (11) and using $D(x) \gg 2\xi_m(t,x)$ and (13) to get $\dot{\xi}(t,x,y)$ yields

$$\iint_{S(BM)} \vec{v}(t,x)\cdot d\vec{S} \approx -\frac{D(x)}{2}\dot{\xi}_m(t,x)\Delta x \quad (14)$$

By substituting (8), (9), (10), and (14) in (7) and letting $\Delta V = S_V(x)\Delta x$, we get the following main equation for the fluid velocity:

$$\nabla[S_V(x)v_V(t,x)] \approx \frac{D(x)}{2}\dot{\xi}_m(t,x). \quad (15)$$

Basilar Membrane Motion

Since we desire the final equations of the model to be expressed in terms of the pressure difference, the fluid velocity, and the geometrical and mechanical parameters of the cochlea, we obtain an independent equation for $\xi_m(t,x)$ from the equation of the BM motion. To set up this equation, we follow [3] and [7] and consider a section of the BM to be a second-order system with an equivalent mass μ, resistance $\sigma(x)$, and stiffness $\phi(x)$, all per unit area. We also use the fact that it is the pressure difference between the two chambers that causes the membrane to deflect at any point. Then, using $\xi_m/2$ as the average displacement over the width $D(x)$, the equation of motion of the BM is

$$-p(t,x) = \mu\frac{\partial^2\xi_m(t,x)/2}{\partial t^2} + \sigma(x)\frac{\partial\xi_m(t,x)/2}{\partial t} + \phi(x)\xi_m(t,x)/2 \quad (16)$$

where the minus sign results from the fact that the pressure difference, p, in the chambers and the average displacement $\xi_m/2$ of the BM have opposite effects. Next we take over time the Laplace transform of (16) with variable s and solve for $D(x)\xi_m(s,x)/2$ as follows:

$$\frac{D(x)\xi_m(s,x)}{2} = -\frac{p(s,x)}{sQ(s,x)} \quad \text{with} \quad Q(s,x) = \frac{\mu s^2 + \sigma(x)s + \phi(x)}{D(x)s}. \quad (17)$$

We let

$$P(s,x) = \frac{2}{S_V(x)}[R_V + \rho_F s] \quad (18)$$

and express the Laplace transforms of (5) and (15) in terms of $P(s,x)$ and $Q(s,x)$ and summarize the results in a matrix form as follows:

$$\nabla\begin{bmatrix} p(s,x) \\ u_V(s,x)\end{bmatrix} = -\begin{bmatrix} 0 & P(s,x) \\ \dfrac{1}{Q(s,x)} & 0\end{bmatrix}\begin{bmatrix} p(s,x) \\ u_V(s,x)\end{bmatrix}. \quad (19)$$

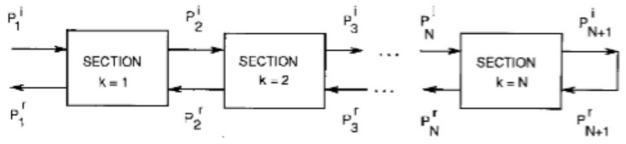

Fig. 2. A cascade of cochlea sections.

III. A Digital Scattering Model of the Ear

Since the Kemp echoes are based on incident and reflected pressure waves in the cochlea, we convert (19) to a scattering formulation. The digital structure we choose to represent the cochlea is a cascade of several digital scattering-based lattices of similar structure, but differing parameters, and where each lattice models a section of the cochlea.

Scattering Treatment

To convert the linear model of (19) to a scattering one, we first split the pressure difference wave p into an incident pressure wave p^i and a reflected pressure wave p^r, then rewrite (19) in terms of these scattering signals. The pressure p and the velocity v_V are related to p^i and p^r via the definition:

$$\begin{bmatrix} p(s,x) \\ u_V(s,x) \end{bmatrix} = \begin{bmatrix} 1 & 1 \\ G(s,x) & -G(s,x) \end{bmatrix} \begin{bmatrix} p^i(s,x) \\ p^r(s,x) \end{bmatrix} \tag{20}$$

where G is the s-domain-valued "conductance" normalization parameter which has G' as its derivative with respect to x. Taking the derivative with respect to x of the right-hand side of (20), equating the result to the RHS of (19), and substituting (20) in (19) yields (21), shown at the bottom of the page.

To make the coefficient matrix of (21) symmetric we choose

$$G^2(s,x) = \frac{1}{P(s,x)Q(s,x)}. \tag{22}$$

On substituting (22) in (21) and defining

$$\rho(s,x) = -\frac{G'(s,x)}{2G(s,x)} = \frac{1}{4P(s,x)Q(s,x)} \cdot \nabla[P(s,x)Q(s,x)] \tag{23}$$

$$\gamma(s,x) = \frac{1}{G(s,x)Q(s,x)} = \sqrt{\frac{P(s,x)}{Q(s,x)}} \tag{24}$$

we rewrite (21) as follows:

$$\nabla \begin{bmatrix} p^i(s,x) \\ p^r(s,x) \end{bmatrix} = \begin{bmatrix} \rho(s,x) - \gamma(s,x) & -\rho(s,x) \\ -\rho(s,x) & \rho(s,x) + \gamma(s,x) \end{bmatrix} \begin{bmatrix} p^i(s,x) \\ p^r(s,x) \end{bmatrix} \tag{25}$$

where $\rho(s,x)$ is similar to a "reflection coefficient" and $\gamma(s,x)$ to a "propagation function" yielding a delay through the section. We note (see the Appendix for details), however, that $\gamma(s,x)$ is negligible compared to $\rho(s,x)$ in the 0–30 kHz range, which contains the Kemp echo dominant frequency range (between 0.5 and 4 kHz) for all the sections. It is, therefore, reasonable to ignore the effect of $\gamma(s,x)$ in this frequency range.

Space Discretization

To derive the desired digital model, as a first step, we represent the model as a cascade of N sections of equal length Δx terminated by a direct connection (modeling the Helicotrema end), since at this end the fluid velocity is zero (Fig. 2). All quantities are indexed with k to denote space discretization. Each section is described by its transfer scattering matrix which relates the incident and reflected pair (p^i, p^r) of a given section (the kth) to the pair (p^i, p^r) of the next section (the $(k+1)$st).

For the space discretization, we consider a section of length Δx, where, for a total of N sections, we have

$$\Delta x = \frac{L}{N}, \qquad x_k = \frac{kL}{N} = x_{k-1} + \Delta x, \qquad k = 1, \cdots, N, \quad x_0 = 0. \tag{26}$$

The discretized equations for the kth section are obtained from (25) by assuming $\gamma(s,x) = 0$, evaluating $\rho(s,x)$ at $x = x_k$, approximating the pressure gradient with a difference, and rewriting (25) as follows:

$$\begin{bmatrix} p^i(s) \\ p^r(s) \end{bmatrix}_{k+1} = \frac{1}{1-\rho_k(s)} \begin{bmatrix} 1 & -\rho_k(s) \\ -\rho_k(s) & 1 \end{bmatrix} \cdot \begin{bmatrix} p^i(s) \\ p^r(s) \end{bmatrix}_k \tag{27}$$

where

$$\rho_k(s) = \rho(s, x_k)\Delta x, \quad [p^i(s,x_k), p^r(s,x_k)] = [p^i(s), p^r(s)]_k. \tag{28}$$

We interchange the two rows in (27), i.e., $p^i_{k+1}(s)$ and $p^r_{k+1}(s)$, and then invert the coefficient matrix to determine the transfer scattering matrix $\theta_k(s)$, (29), for which we show the corresponding signal-flow graph in Fig. 3.

$$\theta_k(s) = \frac{1}{1+\rho_k(s)} \begin{bmatrix} \rho_k(s) & 1 \\ 1 & \rho_k(s) \end{bmatrix}. \tag{29}$$

In (30) we give the expression for $\rho(s, x_k)$ derived from (17), (18), and (23), using the following expressions for the width, area of cross-section, resistance, and stiffness of the cochlea, assuming suitable constants a through K. These expressions are consistent with a number of entries given in Table I.

$$D(x) = ax + b, \quad S_V(x) = ce^{-dx}$$
$$\sigma(x) = fe^{-gx}, \quad \phi(x) = he^{-Kx} \tag{30}$$

$$\rho(s, x_k) = \frac{a_{k2}s^2 + a_{k1}s + a_{k0}}{b_{k2}s^2 + b_{k1}s + b_{k0}} \tag{31}$$

where

$$a_{k2} = \mu[D(x_k)d - a],$$
$$a_{k1} = \sigma(x_k)[D(x_k)d - a - gD(x_k)],$$
$$a_{k0} = \phi(x_k)[D(x_k)d - a - KD(x_k)] \tag{32}$$
$$b_{k2} = 4D(x_k)\mu, \quad b_{k1} = 4D(x_k)\sigma(x_k),$$
$$b_{k0} = 4D(x_k)\phi(x_k) \tag{33}$$

$$\nabla \begin{bmatrix} p^i \\ p^r \end{bmatrix} = -\frac{1}{2G} \begin{bmatrix} G' + P\left(\frac{1}{PQ} + G^2\right) & -G' + P\left(\frac{1}{PQ} - G^2\right) \\ -G' - P\left(\frac{1}{PQ} - G^2\right) & G' - P\left(\frac{1}{PQ} + G^2\right) \end{bmatrix} \begin{bmatrix} p^i \\ p^r \end{bmatrix} \tag{21}$$

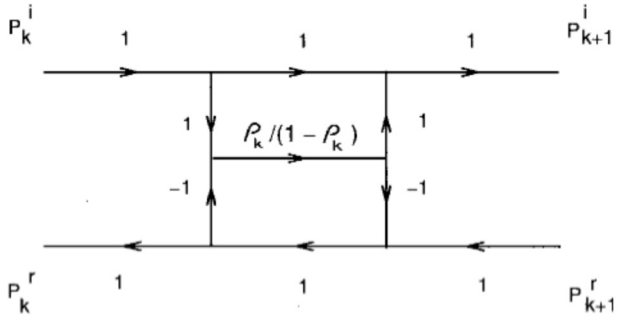

Fig. 3. Signal-flow graph of section k.

Time Discretization

In the second step of the derivation of the digital scattering model, we discretize the time in (29) using the standard bilinear transformation [9, p. 207]

$$s = 2f_s \frac{z-1}{z+1} \tag{34}$$

where $1/z$ is the unit delay, f_s the sampling frequency used on the output signal (Kemp echoes). Using this transformation, the transfer scattering matrix is rewritten as

$$\theta_k(z) = \frac{1}{N_k(z)+D_k(z)} \begin{bmatrix} N_k(z) & D_k(z) \\ D_k(z) & N_k(z) \end{bmatrix} \tag{35}$$

where

$$\frac{N_k(z)}{D_k(z)} = \rho_k(z) = \frac{A_{k2}z^2 + A_{k1}z + A_{k0}}{B_{k2}z^2 + B_{k1}z + B_{k0}} \Delta x \tag{36}$$

with, on using (34) in (31)

$$\begin{aligned} A_{k2} &= 4f_s^2 a_{k2} + 2f_s a_{k1} + a_{k0}, \quad A_{k1} = -8f_s^2 a_{k2} + 2a_{k0} \\ A_{k0} &= 4f_s^2 a_{k2} - 2f_s a_{k1} + a_{k0} \end{aligned} \tag{37}$$

$$\begin{aligned} B_{k2} &= 4f_s^2 b_{k2} + 2f_s b_{k1} + b_{k0}, \quad B_{k1} = -8f_s^2 b_{k2} + 2b_{k0} \\ B_{k0} &= 4f_s^2 b_{k2} - 2f_s b_{k1} + b_{k0}. \end{aligned} \tag{38}$$

IV. Estimation of the Parameters of the Ear

The problem we would like to eventually solve via Kemp echoes is: what are the BM width, damping, and stiffness for a given healthy or damaged ear and how do their x dependencies deviate from what they should be for an equivalent healthy ear? To answer these questions, we first note that in the lattice structure the entries of the transfer scattering matrix of (35) are functions of the A_k and B_k coefficients which, in turn, depend on the width, damping, and stiffness of the BM. To extract these parameters directly from these entries, we use Kemp echo signals collected from normal human ears and provided to us by Dr. H. P. Wit and Dr. P. Van Dijk from the Institute of Audiology (the Netherlands) to determine the transfer scattering matrix of each section through an ARMA filter synthesis technique [4], [10] which allows us to realize the cochlea model as a cascade of 16 degree two-real lattice sections.

With the scattering matrices at hand, we determine [by inspection of (35) and (36)] the A_k and the B_k coefficients. We then calculate the a_k's from (37) and the b_k's from (38) from which the width D, the damping σ, the stiffness ϕ, and the parameters g and K are estimated [(33) and (32)]:

$$D(x_k) = \frac{b_{k2}}{4\mu}, \quad \sigma(x_k) = \mu \frac{b_{k1}}{b_{k2}}, \quad \phi(x_k) = \mu \frac{b_{k0}}{b_{k2}} \tag{39}$$

$$g = 4\left[\frac{a_{k2}}{b_{k2}} - \frac{a_{k1}}{b_{k1}}\right], \quad K = 4\left[\frac{a_{k2}}{b_{k2}} - \frac{a_{k0}}{b_{k0}}\right]. \tag{40}$$

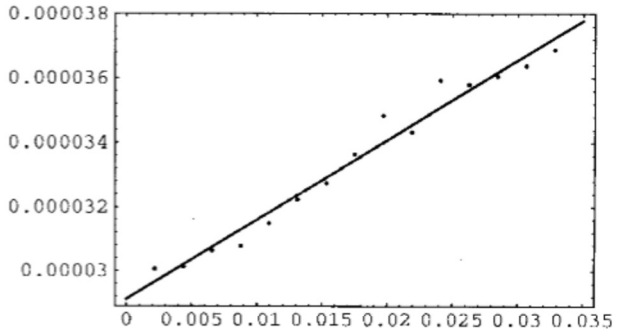

Fig. 4. Width $D(x)$ of the BM as a function of the displacement x along the BM, estimated from Kemp echo data.

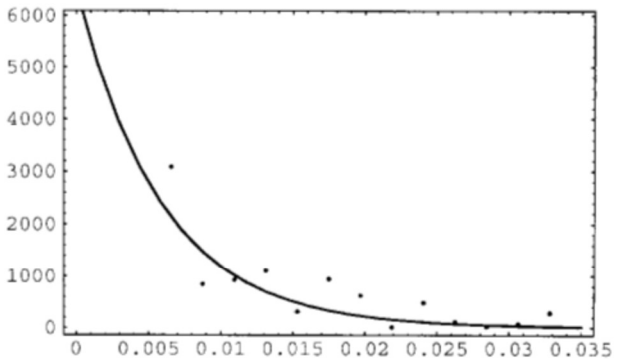

Fig. 5. Damping parameter $\sigma(x)$ of the BM as a function of the displacement x along the BM, estimated from Kemp echo data.

The width $D(x)$, damping $\sigma(x)$, and stiffness $\phi(x)$ of the BM, and the parameters g, and K are evaluated for each of the 16 sections of the cochlea. The values of g and K are found to change very little from section to section and their average values over the 16 sections are 170 m^{-1} and 340 m^{-1}, respectively. The values of $D(x), \sigma(x)$, and $\phi(x)$, however, vary from section to section, being smallest at the first section and increasing linearly for $D(x)$, and largest at the first section and decreasing exponentially for $\sigma(x)$ and $\phi(x)$. Their functional dependency on the displacement x along the BM is obtained by curve fitting the estimated values for each one, using a program such as MATHEMATICA, and assuming (30) as shown in Figs. 4, 5, and 6. The resulting expressions are given explicitly by

$$D(x) = 0.002911 + 0.000248x \text{ cm} \tag{41}$$

$$\begin{aligned} \sigma(x) &= 6500e^{-170x} \text{ N} \cdot \text{s} \cdot \text{m}^{-3} \\ &= 650e^{-1.7x} \text{ dyne} \cdot \text{s} \cdot \text{cm}^{-3} \end{aligned} \tag{42}$$

$$\begin{aligned} \phi(x) &= 1.1\,10^{10}e^{-340x} \text{ N} \cdot \text{m}^{-3} \\ &= 1.1\,10^{9}e^{-3.4x} \text{ dyne} \cdot \text{cm}^{-3}. \end{aligned} \tag{43}$$

The comparison of the expressions of $D(x), \sigma(x)$, and $\phi(x)$ with the ones given in Table I show that $D(x)$ is similar to the width estimated by Peterson in that they are both linear functions of the displacement while $\sigma(x)$ and $\phi(x)$ are similar to the ones estimated by Allen and Zwislocki. The values of $D(x)$ are, however, about one tenth of the values obtained by Peterson, whereas the values of $\sigma(x)$ and $\phi(x)$ have the same order of magnitude as those predicted by Allen and Zwislocki.

V. Discussion and Conclusions

In this brief, we developed the theory for a digital scattering model of the cochlea from a unidimensional transmission line model,

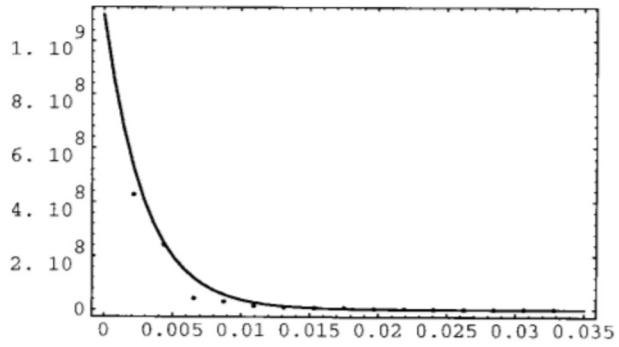

Fig. 6. Stiffness $\phi(x)$ of the BM as a function of the displacement x along the BM, estimated from Kemp echo data.

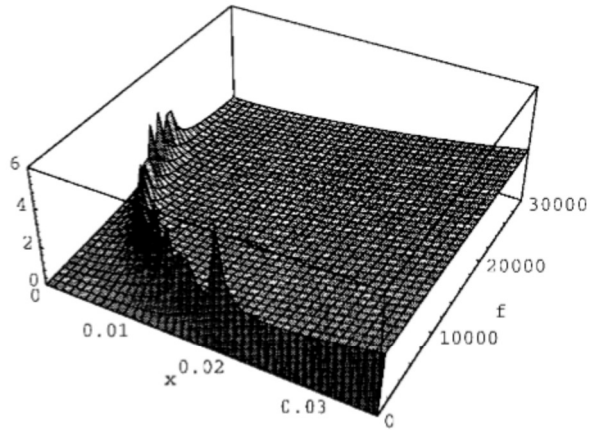

Fig. 7. Magnitude of $|\gamma(f,x)|$ as a function of stimulus frequency f and displacement x along the BM.

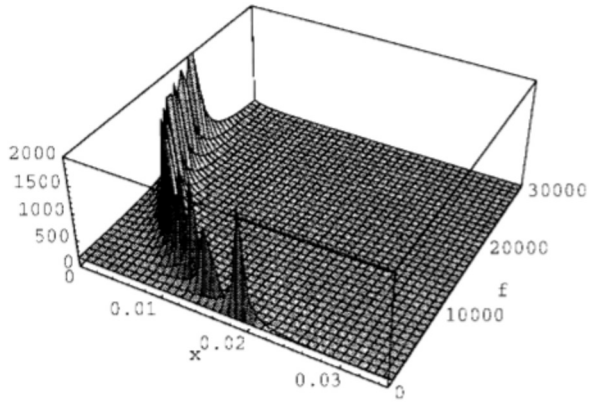

Fig. 8. Magnitude of $|\rho(f,x)|$ as a function of stimulus frequency f and displacement x along the BM.

thus obtaining a pipeline lattice structure. The model and the theory developed are used to characterize the cochlea from noninvasive measurements (Kemp echoes) and should be of particular use in clinical applications for the hearing impaired.

Although we introduced simplifications and neglected nonlinear effects as valid for normal sound amplitude, the proposed model was able to reproduce quantitatively and qualitatively experimental data. Through a digital lattice synthesis technique and an estimation algorithm the width, the damping, and the stiffness of the BM were estimated and established as functions of the displacement. These functions were found to be similar to the ones estimated by Peterson, Allen, and Zwislocki, i.e., linear for the width, and decreasing exponentials for the damping and the stiffness. The estimated width, however, turned out to be a tenth of the one predicted by Peterson. The values of the damping and the stiffness are of the same order of magnitude as the values estimated by Allen and Zwislocki.

The difference should be noticed between our theory and the classical theory for modeling the cochlea by a cascade of filters whose resonant frequencies are considered to be local tunings of the cochlea. In our case we proceed in the time domain from the transient response (Kemp echo) due to a sharp input pressure pulse to the oval window. This has theoretical advantages in that all frequencies are taken into account, media parameters are directly estimated, and extensions to nonlinear models readily made; the main disadvantage is that considerable care is needed in the measurements, which are of low intensities and where isolation of signals from noise is a concern.

The mathematical equations of the model were derived assuming several geometrical and mechanical simplifications, some of which will now be examined. The cochlea has several leaks, situated at its base, which allow communication with the vestibular cavity. Therefore, assuming that the cochlea is an isolated cavity is not totally realistic near the base, since the fluid movement in the vestibular cavity would affect the movement of the fluid in the cochlea and, thus, the BM vibrations. However, far from the base of the cochlea, the effect of the simplification upon the BM is probably small. It has been shown [11] that the effect of the compressibility of the fluid is negligible in the low and mid-frequency range, and can have at most a minor influence at the highest audio-frequencies. Since the dominant frequencies of Kemp echoes are measured in the range extending from 0.5 to 4 kHz [12], the fluid incompressibility assumption is therefore reasonable for our model. The extent to which the spiral shape affects the BM motion was analyzed by Viergever [13] using data from human ears. The analysis showed that the mechanical behavior of the cochlea was affected only slightly by the spiral form, even near the apex where the coiling is very tight.

As pointed out by the reviewers, the analysis of the robustness of the model with respect to poor estimation of its input parameters is very important. In fact, Kemp echo signals, which are used here to estimate the width, damping, and stiffness of the basilar membrane, are subject to a relevant degree of uncertainty. In addition to noise, experimental evidence shows that these echoes differ from ear to ear and change with the stimulus amplitude and frequency. Therefore, the quantification of the sensitivities of the estimated parameters to both poor measurements in Kemp echoes and their deviation from ear to ear should prove valuable clinically, as, for instance, in setting up thresholds for use in hearing screening and the diagnosis of hearing loss. A preliminary investigation revealed the sensitivity analysis to be rather complex and lengthy and, thus, will be the subject of a future study.

As can be appreciated from the complexity of the ear, it is expected that the incorporation of nonlinearities inherent to the BM, micromechanical coupling to the tectorial membrane, and hair cells will lead to better models for explaining the generation of spontaneous and evoked oto-acoustic emissions. Our cascaded digital lattice structure lends itself very well to both nonlinear and lossy transformations. Furthermore, because of the scattering nature of the model, it can be upgraded to a two-channel model by splitting up the pressure wave into two pairs of incident and reflected waves, one for each channel, and model each section of the cochlea by a four-port system, as initiated by Chang [14], instead of a two-port lattice as used here. Finally, it should be noted that to preserve the cross-sectional area parameter $S_V(x)$ present in $\gamma(s,x)$, other synthesis methods can be developed to handle a lattice structure of the type given in (25).

APPENDIX

We base the assumption $\gamma(s,x) \ll \rho(s,x)$, made in Section III, on (24) and (31)–(33), and evaluate $\gamma(s,x)$ and $\rho(s,x)$, using Table I for $L, \rho_F, \mu, D(x)$ (Peterson), $S_V(x)$ (Zwislocki), $\sigma(x)$ (Allen), $\phi(x)$ (Allen) and $R_V = 56\,\mathrm{kg/m^3 s}$ (needed only to evaluate $\gamma(s,x)$) [7]. We set $s = j2\pi f$ in (24) and (31) and plot $|\gamma(f,x)|$ and $|\rho(f,x)|$ versus frequency (in the range 0–30 kHz) and displacement along the cochlea. These plots (Figs. 7 and 8) show that, at any position along the cochlea, $|\gamma(f,x)|$ and $|\rho(f,x)|$ are similar to the frequency response of a highly tuned filter. The resonant frequency is higher near the base of the cochlea and decreases toward the apex. The lowest value of $|\rho(f,x)|$ in the stop-band region is 40 while the highest value of $|\gamma(f,x)|$ is 1.5, which makes ρ at least 25 times larger than γ. At resonance, the smallest peak of $|\rho(f,x)|$ is approximately 600, whereas the highest peak of $|\gamma(f,x)|$ is 6, which makes ρ at least 100 times larger. Therefore, in light of these results, it is reasonable to ignore $\gamma(s,x)$ in (25).

REFERENCES

[1] D. T. Kemp, "Stimulated acoustic emissions from within the human auditory system," *J. Acoust. Soc. Amer.*, vol. 64, no. 5, pp. 1386–1391, Nov. 1978.

[2] H. P Wit and R. J. Ritsma, "Evoked acoustical responses from the human ear: Some experimental results," *Hearing Res.*, vol. 2, pp. 253–261, 1980.

[3] P. Gomez Vilda, "Modelo incremental recursivo para el analisis de la mecanica del oido medio e interno," Doctoral dissertation, Facultad de Inform. Univ. Politec. Madrid, Spain, 1982.

[4] L. Sellami, "Kemp echo lattices incorporating hair cell nonlinearities," Doctoral dissertation, Electrical Engineering, University of Maryland, 1992.

[5] P. Gomez, V. Rodellar, and R. W. Newcomb, "A digital lattice for cochlear parameter identification," in *Proc. IV Mediterranean Conf. Medical Biomed. Eng.*, Sept. 1986, pp. 637–640.

[6] ——, "Kemp echo digital filters," in *Proc. First Int. Conf. Advances in Commun. Contr. Syst.*, June 1987, pp. 38–46.

[7] R. W. Newcomb, "Notes on cochlear models for Kemp echoes," Tech. note, Univ. Maryland, Dec. 1988.

[8] B. Munson, D. Young, and T. Okiishi, *Fundamentals of Fluid Mechanics*. New York: Wiley, 1990.

[9] A. V. Oppenheim and R. W. Schafer, *Digital Signal Processing*. Englewood Cliffs, NJ: Prentice-Hall, 1975.

[10] L. Sellami and R. W. Newcomb, "Synthesis of ARMA Filters by Real Lossless Digital Lattices," *IEEE Trans. Circuits Syst. II*, vol. 43, pp. 379–386, May 1996.

[11] G. Zweig, "Finding the impedance of the organ of corti," *J. Acoust. Society Amer.*, vol. 89, no. 3, pp. 1229–1254, Mar. 1991.

[12] J. C. Langevoort, H. P Wit, and R. J. Ritsma, "Frequency spectra of cochlear acoustic emissions," *J. Acoust. Soc. Amer.*, vol. 70, pp. 437–445, 1981.

[13] M. A. Viergever, "Basilar membrane motion in a spiral-shaped cochlea," *J. Acoust. Soc. Amer.*, vol. 64, no. 4, pp. 1048–1053, Oct. 1978.

[14] T. Cheng, "Realization of transmission lattice filters," Doctoral dissertation, Electrical Eng., Univ. Maryland, 1990.

Intermodulation Noise Related to THD in Wide-Band Amplifiers

Henrik Sjöland and Sven Mattisson

***Abstract*—In this brief, it is shown that the power of the intermodulation noise of a wide-band amplifier with a Gaussian input signal, can be estimated by the total harmonic distortion (THD) with a sinusoid input signal of appropriate amplitude. The THD is, as opposed to the intermodulation noise, easy to measure and use as a design parameter. A novel method based on probability density functions is used. The method is demonstrated by a practical example, and a mathematical experiment is made to validate it.**

I. INTRODUCTION

Intermodulation occurs when two or more signals at different frequencies passes a nonlinearity. The intermodulation products (noise) of a wide-band signal are very complex, since the signal contains an infinite number of frequency components. When designing a wide-band amplifier, it is necessary to have an estimate of the linearity required to keep the intermodulation below a certain level. The complex intermodulation, therefore, has to be related to something that is easier to use as a design parameter. The total harmonic distortion THD is a common measure of nonlinearity, and is in this paper related to the intermodulation power. THD is defined as the ratio of the total energy in the harmonics and the energy in the base signal, when a single sinusoid is applied, see for example [1, pp. 18–27].

We assume that the input signal amplitude is normal distributed. This is true for Gaussian noise and it is a good approximation when several similar uncorrelated random signals are added, such as a number of radio channels of similar power. Another approximation made is that all the intermodulation noise power will be in the working band of the wide-band amplifier. If the bandwidth is large enough this is a good approximation.

Let x be the input and $f(x)$ the output of an amplifier. To model clipping we assume:

$$f(x) = \begin{cases} f(1) & x > 1 \\ x + a_2x^2 + a_3x^3 \cdots & |x| \le 1 \\ f(-1) & x < -1 \end{cases} \tag{1}$$

The characteristic is normalized such that the gain and the largest input signal amplitude before clipping equals one, see Fig. 1.

II. TIME INTEGRAL FORMULATION

Assume that THD is measured for an input signal $x = A\sin(t)$. Let the nonlinearity be represented by

$$g(x) = a_2x^2 + a_3x^3 + \cdots. \tag{2}$$

The total power due to the nonlinear terms $g(x)$ is then

$$P_T = \frac{1}{2\pi}\int_0^{2\pi} g[x(t)]^2\,dt. \tag{3}$$

Manuscript received August 7, 1995; revised March 7, 1996. This work was supported by the Swedish National Board for Industrial and Technical Development (NUTEK). This paper was recommended by Associate Editor A. Ushida.

The authors are with the Department of Applied Electronics, Lund University, S-221 00 Lund, Sweden.

Publisher Item Identifier S 1057-7122(97)01498-0.